Slow epidemic extinction in populations with heterogeneous infection rates

C. Buono,[1] F. Vazquez,[2,3] P. A. Macri,[1] and L. A. Braunstein[1,4]

[1]*Instituto de Investigaciones Físicas de Mar del Plata UNMdP-CONICET and Departamento de Física FCEyN, Universidad Nacional de Mar del Plata, Funes 3350 (7600) Mar del Plata, Argentina*

[2]*Max-Planck-Institut für Physik Komplexer Systeme Nöthnitzer Str. 38, D-01187 Dresden, Germany*

[3]*Instituto de Física de Líquidos y Sistemas Biológicos UNLP-CONICET, Calle 59 Nro 789 (1900), La Plata, Argentina*

[4]*Center for Polymer Studies, Boston University, Boston, Massachusetts 02215, USA*

(Received 19 December 2012; published 26 August 2013)

We explore how heterogeneity in the intensity of interactions between people affects epidemic spreading. For that, we study the susceptible-infected-susceptible model on a complex network, where a link connecting individuals i and j is endowed with an infection rate $\beta_{ij} = \lambda w_{ij}$ proportional to the intensity of their contact w_{ij}, with a distribution $P(w_{ij})$ taken from face-to-face experiments analyzed in Cattuto *et al.* [PLoS ONE **5**, e11596 (2010)]. We find an extremely slow decay of the fraction of infected individuals, for a wide range of the control parameter λ. Using a distribution of width a we identify two large regions in the a-λ space with anomalous behaviors, which are reminiscent of rare region effects (Griffiths phases) found in models with quenched disorder. We show that the slow approach to extinction is caused by isolated small groups of highly interacting individuals, which keep epidemics alive for very long times. A mean-field approximation and a percolation approach capture with very good accuracy the absorbing-active transition line for weak (small a) and strong (large a) disorder, respectively.

DOI: 10.1103/PhysRevE.88.022813 PACS number(s): 89.75.Hc, 02.50.Ey, 05.40.−a, 87.19.X−

I. INTRODUCTION

Nowadays, much of daily human activity is constantly being recorded by means of modern technologies, such as Internet, GPS, mobile phones, bluetooth, and other electronic devices. The gathering and analysis of large amounts of activity data have allowed the exploration of statistical features of people's behavior. In particular, recent studies have revealed interesting properties about how humans interact with each other, either by having conversations [1], or sexual contacts [2], or by means of mobile devices [3] or wireless communications [4]. Despite the fact that the type of interactions in these studies are quite different, they all found a common interaction pattern, that is, human contacts are very heterogeneous. This is consistent with a broad distribution of different magnitudes that quantify the timing of contacts, such as their duration, frequency, and gaps. This diversity could eventually have an impact on propagation processes that involve human contact, such as the spreading of rumors or diseases.

In this article we explore epidemic spreading on a population with heterogeneous interaction intensities. We use a distribution of intensities extracted from the pattern of contacts between participants of a conference [5], obtained in recent face-to-face experiments [1]. For the spreading process we use the susceptible-infected-susceptible (SIS) [6] dynamics on Erdős-Rényi (ER) networks [7], with infection rates across links that are proportional to the intensity of encounters.

As the rate of infection increases, the original SIS model [6] exhibits a transition from an absorbing (disease-free) phase where the infection dies exponentially fast to an active (endemic) phase where the infection spreads over a large fraction of the population and becomes persistent. We find that the heterogeneity in the intensity of contacts introduces an intermediate absorbing region, in which the epidemic dies very slowly, as a stretched exponential or a power law in time. We experiment with other rate distributions and show that this slow approach to epidemic extinction is caused by the presence of small clusters composed by links with high infection rates, which remain infected for very long times. We also discuss analogies with the effects observed in models with quenched disorder [8].

While our results are mainly concerned with the decay of the infection in the epidemic-free phase, some related models [9–11] have focused, instead, on the disease prevalence within the endemic phase, or study the spreading power of a given node [12] using the susceptible-infected-recovered dynamics. Other studies have introduced heterogeneity at the individual level, by assigning power-law intertime events [13,14], node-dependent infection rates [15], or topology-dependent weight patterns [16–18]. In our model heterogeneity is at the interaction level, by means of link-dependent infection rates, which are not correlated with the topology of the network.

II. SIS DYNAMICS WITH FACE-TO-FACE DISORDER

In the SIS model [6], each individual of a population can be either susceptible (healthy) or infected. Infected individuals transmit the disease to its susceptible neighbors in the network at a rate ν and return to the susceptible state at a rate γ. The dynamics is controlled by the rescaled infection rate $\lambda = \nu/\gamma$. For λ above a critical value λ_c, even a small initial fraction of infected nodes is able to propagate the disease through the entire network (active phase), while for $\lambda < \lambda_c$ the disease quickly dies out (absorbing phase), following an exponential decay in the number of infected nodes.

This model describes disease spreading in an ideal population where transmission rates between individuals are all the same. However, in real populations we expect interactions to be heterogeneous, having a broad range of intensities, as recently measured by analyzing mobile phone data [3] and by means

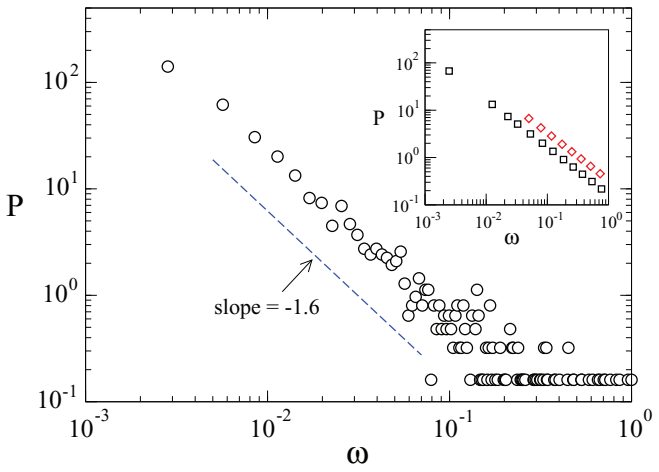

FIG. 1. (Color online) Probability distribution of face-to-face contacts intensities (weights w) of the 25th Chaos Communication Conference in Berlin, on a log-log scale. Intensity is defined as the total number of packages exchanged between two attendees, which is proportional to the contact duration. The large dispersion of the data reflects the large heterogeneity in the duration of contacts. Weights are rescaled to the interval $[0,1]$ for a better comparison with the theoretical distribution $P(w) = 1/aw$ in the interval $[e^{-a},1]$, as shown in the inset for $a = 6$ (squares) and $a = 3$ (diamonds).

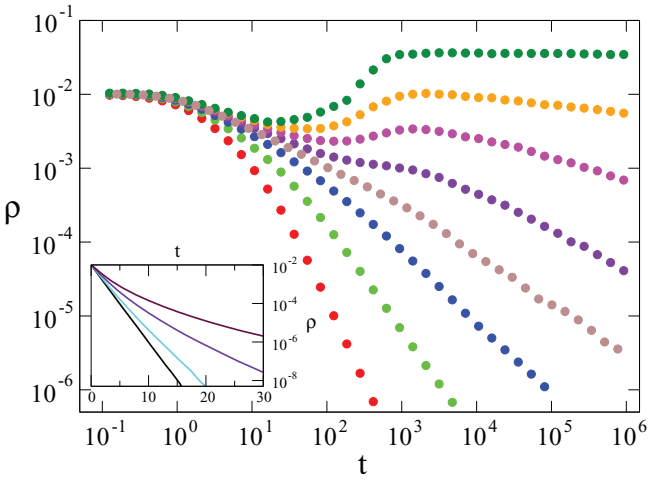

FIG. 2. (Color online) Average density of infected nodes ρ vs time t, on a log-log scale, under the SIS dynamics on ER networks with $\langle k\rangle = 4$ and $N = 10^5$ nodes. The infection rate distribution $P(\beta)$ corresponds to the weight distribution $P(w)$ of Fig. 1, with $\beta = \lambda w$, for values of the control parameter $\lambda =$ 3.9,3.7,3.6,3.5,3.4,3.3,3.0,2.5 (main plot) and $\lambda =$ 1.5,1.0,0.5,0.2 (inset), from top to bottom. ρ decays as a power law for $2.0 \lesssim \lambda \lesssim 3.7$, as a stretched exponential for $0.25 \lesssim \lambda \lesssim 2.0$, and as an exponential for $\lambda \lesssim 0.25$, as shown in the inset on a linear-log scale.

of person-to-person experiments [1]. In order to explore how the behavior of the SIS model is affected by the heterogeneity of interactions, we run simulations of the dynamics on ER networks with infection rates distributed according to the weight distribution $P(w)$ of face-to-face experiments [1,5] (see Fig. 1). In these experiments, participants of a three-day conference were asked to wear a radio frequency identification device on their chest, so that when two persons were close and facing each other a relation of face-to-face proximity was registered. The weights w of Fig. 1 are defined as the total number of packets exchanged (or total contact time) between pairs of participants during the three days.

We are assuming that infection rates are proportional to the total time individuals are in contact with each other, as the likelihood of transmission increases with exposure time; longer contacts imply a higher risk of infection. Therefore, we assign an effective rate of infection $\beta_{ij} = \lambda w_{ij}$ between two individuals i and j that are connected by a link of weight w_{ij}, where λ is a free parameter that acts as a transformation scale of contact intensities into infection rates.

In Fig. 2 we show simulation results of the time evolution of the average density of infected individuals ρ, over many realizations of the SIS dynamics, starting from a configuration where a small fraction of nodes have been randomly infected, and with infection rates following the distribution of Fig. 1. All simulations in this article correspond to ER networks of mean degree $\langle k\rangle = 4$ and $N = 10^5$ nodes. We understand that ER networks are an oversimplification of the complex topology of interaction between attendees at the Berlin's conference, which is known to have a broad degree distribution peaked at an intermediate value (similar to a Poissonian) as well as topological and temporal correlations due to the intricate pattern of contacts [19]. However, ER networks, which have a Poisson degree distribution but are uncorrelated, are simple enough to allow for an exploration of the effects of the heterogeneity in the interaction strengths, avoiding other possible effects due to its specific degree distribution and correlations.

We found that, besides the typical behavior observed in the active and exponential phases of the classic SIS model (all infection rates are the same), there is an intermediate region between $\lambda = 0.25$ and 3.7 with very slow relaxation to the absorbing state. The region $2.0 \lesssim \lambda \lesssim 3.7$ is characterized by a power-law decay with a continuously varying exponent, while in the region $0.25 \lesssim \lambda \lesssim 2.0$ the decay is faster than a power law but slower than exponential (see the inset of Fig. 2), and can be fitted by a stretched exponential.

III. SIS DYNAMICS WITH VARIABLE DISORDER STRENGTH

In order to understand this phenomenon we explore the dynamics for different distributions of weights. We assign to each link ij a weight $w_{ij} = e^{-ar_{ij}}$, where r_{ij} is a random number taken from a uniform distribution in the interval $[0,1]$, and a is a parameter that sets the range of w_{ij} in $[e^{-a},1]$. This method generates a power-law distribution $P(w) = 1/aw$. The parameter a controls the width of the distribution, and measures the heterogeneity or strength of disorder. In the inset of Fig. 1 we plot $P(w)$ for $a = 6$ and $a = 3$, which is intended to mimic the broad distribution of face-to-face contacts, even though the decay exponents are different.

The distribution of infection rates is given by

$$P(\beta) = \frac{1}{a\beta}, \quad \text{with} \quad \beta \text{in}[\lambda e^{-a},\lambda]. \tag{1}$$

Notice that when $a \to 0$ we recover the classic model where $\beta_{ij} = \lambda$ for all ij. This kind of disorder was already used in

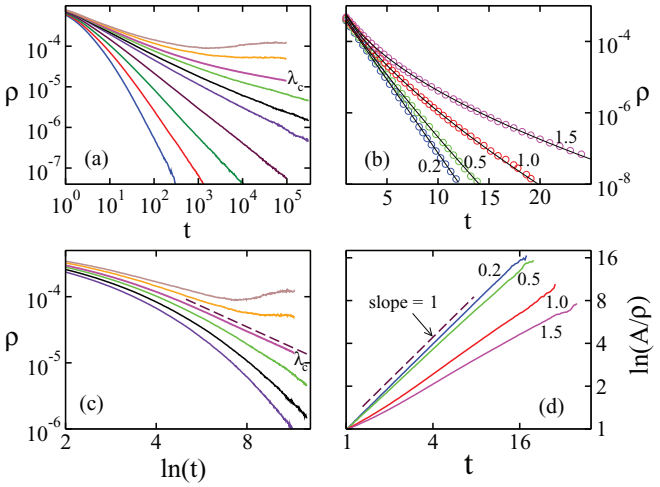

FIG. 3. (Color online) SIS dynamics on ER networks with $\langle k\rangle = 4$, $N = 10^5$ and distribution of infection rates $P(\beta) = 1/a\,\beta$, with $a = 20$ and β in $[\lambda e^{-a},\lambda]$. (a) ρ vs time on a double logarithmic scale, for $\lambda = 6.0,5.8,\lambda_c \simeq 5.56,5.4,5.2,5.0,4.5,4.0,3.5$ and 3.0 (from top to bottom). ρ decays as a power law for $2.0 \lesssim \lambda \lesssim \lambda_c$. (b) ρ vs time on a linear-log scale, for $\lambda = 0.2,0.5,1.0$ and 1.5 (circles). Straight lines are best fittings using the function $A\,e^{-\alpha t^b}$ with $A = 0.0009735$, $\alpha = 0.94731$, $b = 1.0$ for $\lambda = 0.2$; $A = 0.0016$, $\alpha = 1.21$, $b = 0.86$ for $\lambda = 0.5$; $A = 0.0028$, $\alpha = 1.61$, $b = 0.69$ for $\lambda = 1.0$; and $A = 0.0045$, $\alpha = 2.03$, $b = 0.54$ for $\lambda = 1.5$. Only $\lambda = 0.2$ is in the exponential region $\lambda < 0.25$, while the other curves are stretched exponentials. (c) ρ vs $\ln t$ on a log-log scale, showing the extremely slow decay $\rho \sim (\ln t)^{-\beta}$ at the active-absorbing transition point λ_c. (d) The stretched exponential behavior for $\lambda = 0.5,1.0$ and 1.5 is shown as a straight line by plotting $\ln(A/\rho)$ vs time on a log-log scale.

several works on complex networks [20–22]. We expect that high-weight links facilitate the spreading of infections in our model, while low-weight links hinder the spreading.

The behavior of ρ under the theoretical disorder given by Eq. (1) is very similar to the one observed in Fig. 2 for the face-to-face disorder, showing a slow relaxation to the absorbing state, as we can see in Figs. 3(a) and 3(b). This suggests that the effect of disorder is quite robust, since results seem to be independent on the power-law exponent of the distribution of weights. In the a-λ phase diagram of Fig. 4 we summarize the different types of behaviors. Above the numerical transition line $\lambda_c^{\rm num}(a)$ denoted by the red circles we find the *active phase* (white), where ρ reaches a stationary value larger than zero, and below we find the *absorbing phase* where ρ decays to zero. The transition line corresponds to the value of λ for which the decay is algebraic in the logarithm of time, $\rho \sim (\ln t)^{-\beta}$ [8], as shown in Fig. 3(c). The absorbing phase is divided into three regions. The *exponential region* (green), which appears for $\lambda < \lambda_c^0$, characterized by the decay $\rho \sim e^{-\alpha t}$ of the classic model [see Figs. 3(b) and 3(d)], the *weak effects region* (yellow) where we observe an stretched exponential behavior $\rho \sim A\,e^{-\alpha t^b}$ ($b < 1.0$) [see Figs. 3(b) and 3(d)], and the *strong effects region* (orange), with a power-law decay $\rho \sim t^{-\gamma}$ [see Fig. 3(a)]. Exponents α, b, and γ vary continuously with λ and a. Along the line separating the weak and strong effects regions, we observe a crossover between the pure stretched exponential and power-law decays.

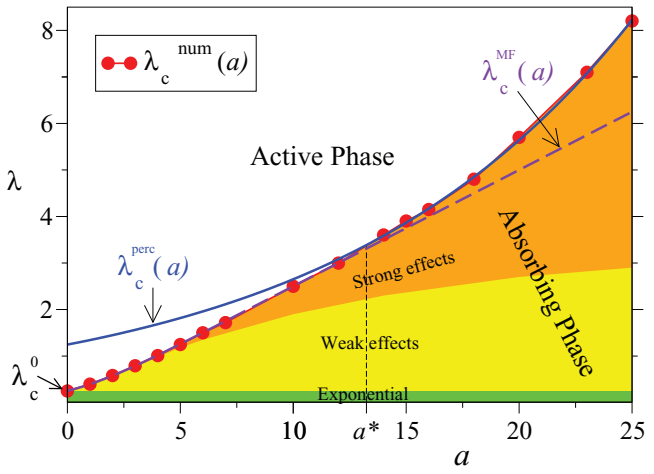

FIG. 4. (Color online) Phase diagram of the SIS model with infection rate distribution $P(\beta) = 1/a\,\beta$, and β in $[\lambda e^{-a},\lambda]$. Colored regions correspond to the absorbing phase: orange and yellow for the strong and weak effects regions, and green for the exponential decay region. The dashed and solid lines are the MF [Eq. (2)] and percolation [Eq. (5)] approximations, respectively, for the transition between the active and absorbing phases.

A. Active-absorbing transition line: mean-field and percolation approaches

In order to gain an insight about the dynamics of the model we develop in this section a theoretical estimation of the transition line between the active and absorbing phases of Fig. 4. Within a mean-field (MF) approximation, ρ evolves according to $\dot\rho = -\rho + \lambda\langle w\rangle\langle k\rangle\rho(1-\rho)$, where $\lambda\langle w\rangle = \lambda(1-e^{-a})/a$ is the average infection rate, and $\langle k\rangle(1-\rho)$ is the average number of susceptible neighbors of an infected node. The stationary solutions $\rho = 0$ and $\rho = (\lambda - \lambda_c^{\rm MF})/\lambda$ correspond to the absorbing and active phases, respectively, with the transition point at

$$\lambda_c^{\rm MF}(a) = \frac{a}{\langle k\rangle(1-e^{-a})}. \tag{2}$$

For $a = 0$ we recover the classic transition point $\lambda_c^0 \equiv \lambda_c$ $(a = 0) = 1/\langle k\rangle = 0.25$ of the classic model. Impurities, in the form of low-weight links, locally reduce infection rates, thus the transition happens at a value $\lambda_c^{\rm MF}(a) > \lambda_c^0$.

Expression (2) (dashed line in Fig. 4) is a very good estimate of $\lambda_c^{\rm num}(a)$ for $a \lesssim 14$ (weak disorder), but systematic deviations appear as a increases. Discrepancies arise because MF assumes that all links can spread the disease but, when a is large, a fraction of links have such small rates (inactive links) that infection never passes through them during the epidemic's life time, and thus the effective network for the spreading dynamics is diluted with respect to the original network. When dilution is large enough the effective network gets fragmented into many small disconnected components and, as the disease cannot spread out of these components the active state is never reached. Therefore, the active-absorbing transition point for a large (strong disorder) corresponds to the *percolation threshold*. This occurs when the fraction of inactive nodes q (nodes attached only to inactive links) exceeds the critical value q_c. For ER networks with Poisson degree

distribution $P_k = e^{-\langle k\rangle}\frac{\langle k\rangle^k}{k!}$ is

$$q = \sum_k l_I^k P_k = e^{-\langle k\rangle(1-l_I)}, \tag{3}$$

where

$$l_I \equiv \int_{\lambda e^{-a}}^{\beta_m} P(\beta)\, d\beta = \frac{1}{a}\ln\left(\frac{\beta_m e^a}{\lambda}\right) \tag{4}$$

is the fraction of inactive links, and β_m is the largest infection rate that does not allow the transmission of the disease. At the percolation threshold $\langle k\rangle = (1-q_c)^{-1}$ in the $N\to\infty$ limit, thus $q_c = \exp\{(1-q_c)^{-1}[\ln(\beta_m\, e^a/\lambda_c^{\rm perc})/a - 1]\}$, from where the percolation transition line is

$$\lambda_c^{\rm perc}(a) = \beta_m\, q_c^{-a(1-q_c)}. \tag{5}$$

Using $q_c = 0.7443$ for a network of size $N = 10^5$ [23], expression (5) with $\beta_m \simeq 1.2457$ is in excellent agreement with $\lambda_c^{\rm num}(a)$ for $a \gtrsim 14$ (solid line in Fig. 4). The value of β_m is estimated from the crossover conditions $\lambda_c^{\rm MF}(a) = \lambda_c^{\rm perc}(a)$ and $\partial\lambda_c^{\rm MF}(a)/\partial a = \partial\lambda_c^{\rm perc}(a)/\partial a$ between the MF and percolation lines at the weak-strong disorder crossing point $a = a^*$. We obtain $\beta_m = -[e\ln q_c]^{-1}$ and $a^* = -[(1-q_c)\ln q_c]^{-1}$ with $a^* \simeq 13.243$ for the network used here.

In the next section we analyze in more detail the dynamics in the absorbing phase and provide an explanation about the origin of slow relaxations.

B. Anomalous behavior in the absorbing phase

We have seen that the heterogeneity in infection rates induces a large new region inside the absorbing phase, in which the temporal evolution of ρ exhibits an anomalous slow decay. This is caused by the presence of exponentially small isolated regions in the network where the system is locally active, that is, with infection rates $\beta_{ij} > \lambda_c^0$, which are able to sustain the activity for very long times. To check this, we calculated the size distribution of clusters composed only by infected nodes $n_I(s)$, at a fixed large time. Results are shown in Fig. 5 for $a = 6$. Inside the weak and strong effects regions ($\lambda = 0.75$ and 1.4), $n_I(s)$ is close to an exponential, and the size of the largest cluster $s_{\rm max}$ is much smaller than the network size $N = 10^5$ (see inset of Fig. 5). Also, the values 0.27 and 0.70 of the average infection rates inside these clusters for $\lambda = 0.75$ and 1.4, respectively, show that the long-time activity is located inside active clusters, in which the average rate of infection $\langle\beta\rangle > \lambda_c^0$. For comparison, in the active phase ($\lambda = 2.0$) is $7600 \lesssim s_{\rm max} \lesssim 9500$, indicating the spreading of the disease over a large fraction of the network.

Similar anomalous behaviors are found in models with disorder, giving rise to the so-called Griffiths phases (GP) [8,15–18,24,25]. The combination of exponentially rare regions in space that survive for exponentially long times results in an overall slowing down of the dynamics, as we show below. The long-time contribution of active clusters to ρ is estimated as

$$\rho \sim \int ds\, s\, P(s)\, e^{-t/\tau(s)}, \tag{6}$$

where $P(s) \sim e^{-\tilde{p}s}$ [26] is the fraction of active clusters of size s and $\tau(s)$ is the mean decay time of those clusters. By doing a saddle-point analysis, and using the finite-size scaling $\tau(s) \sim e^{cs}$, one arrives to the power-law decay $\rho \sim t^{-\tilde{p}/c}$ (with logarithmic corrections) observed in the strong effects region of Fig. 4. The size of active clusters is of order one for λ just above λ_c^0, leading to exponentially weak effects of the form $\rho \sim e^{-\alpha t^b}$ [8].

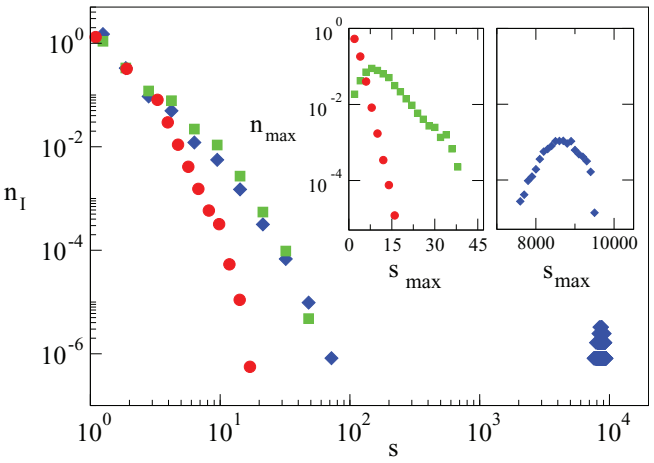

FIG. 5. (Color online) Cluster size distribution of infected nodes n_I for $a = 6$ and values of λ inside three different regions of Fig. 4: $\lambda = 0.75$ (circles) and 1.4 (squares) in the weak and strong effects regions, and 2.0 (diamonds) in the active phase. Distributions correspond to snapshots of the network at fixed large times. The average infection rates inside each cluster are $\langle\beta\rangle \simeq 0.27$, 0.70, and 0.75 for $\lambda = 0.75$, 1.4, and 2.0, respectively. Insets: size distribution of the largest cluster $n_{\rm max}$ showing the appearance of a large component in the active phase.

IV. DISCUSSION AND CONCLUSIONS

In summary, the heterogeneity in the intensity of contacts between individuals induces a regime with extremely slow (power-law or stretched exponential) relaxation to epidemic extinction, akin to the slowing down found in systems with quenched disorder. This effect is very robust, as it was observed using an empirical distribution of contact durations in face-to-face experiments, as well as a theoretical distribution with variable width. Given that both are long-tailed distributions but with different exponents, we suspect that the anomalous relaxation is observed in general for broad weight distributions. To check this concept we run simulations (not shown) using a bimodal distribution $P(\beta) = p\,\delta(\beta-\beta_1) + (1-p)\,\delta(\beta-\beta_2)$, with $0 \leqslant p \leqslant 1$ and $\beta_2 > \beta_1$ [8]. We observed slow relaxations for $\beta_2 > \lambda_c^0 > \beta_1$, that is, when there are finite fractions of links with infection rates above and below the classic transition point λ_c^0.

In order to explore whether these effects depend on the specific topology of interactions, we have done some testing with scale-free networks. We found that the active-absorbing transition line on the phase diagram of Fig. 4 is shifted down to very small values, but we could not clearly identify a finite region with slow decay. Therefore, we suspect that rare-region effects are not present in networks with heterogeneous degree distributions. This is probably because weights are randomly distributed over the network, thus high-degree nodes always

spread the disease (it is very unlikely that all links attached to hubs have very low weights). Instead, assigning weights according to the topology of the network may induce rare-region effects, as it was shown in [16–18] using Barabasi-Albert trees with disassortative weighting. It would be worthwhile to perform a deeper analysis to study how relaxations are affected by other properties of real contact networks, such as topological and temporal correlations.

While temporal heterogeneity, causality, and bursty activity was found to hinder spreading [11,14], we showed here that spatial heterogeneity has the counterbalanced effect, making the epidemic more persistent by slowing down its extinction. Once a group of highly interacting individuals gets infected, they are able to continuously reinfect each other at a high rate, keeping the infection inside the group for very long times. Our findings can be used to design efficient mitigation strategies for the disease. For instance, moderating the activity of highly interacting people could dramatically speed up the final stage of the epidemic.

ACKNOWLEDGMENT

This work was financially supported by UNMdP and FONCyT (Pict 0293/2008). The authors thank Lucas D. Valdez for useful comments and discussions.

[1] C. Cattuto, W. V. den Broeck, A. Barrat, V. Colizza, J.-F. Pinton, and A. Vespignani, PLoS ONE **5**, e11596 (2010).
[2] B. Foxman, M. Newman, B. Percha, K. Holmes, and S. Aral, Sex. Transm. Dis. **33**, 209 (2006).
[3] T. Karagiannis, J.-Y. L. Boudec, and M. Vojnovic, Mobicom **07**, 183 (2007).
[4] A. Scherrer, P. Borgnat, E. Fleury, J.-L. Guillaume, and C. Robardet, Comput. Network. **52**, 2842 (2008).
[5] http://people.openbeacon.org/meri/openbeacon/sputnik/data/25c3
[6] N. T. J. Bailey, *The Mathematical Theory of Infectious Diseases* (Griffin, London, 1975).
[7] P. Erdős and A. Rényi, Publications Mathematicae **6**, 290 (1959).
[8] T. Vojta, J. Phys. A: Math. Gen. **39**, R143 (2006).
[9] J. Stehlé *et al*., BMC Medicine **9**, 87 (2011).
[10] Z. Yang and T. Zhou, Phys. Rev. E **85**, 056106 (2012).
[11] M. Karsai, M. Kivelä, R. K. Pan, K. Kaski, J. Kertész, A.-L. Barabási, and J. Saramäki, Phys. Rev. E **83**, 025102(R) (2011).
[12] A. Garas, P. Argyrakis, C. Rozenblat, M. Tomassini, and S. Havlin, New J. Phys. **12**, 113043 (2010).
[13] A. Vazquez, B. Rácz, A. Lukács, and A.-L. Barabási, Phys. Rev. Lett. **98**, 158702 (2007).
[14] B. Min, K.-I. Goh, and A. Vazquez, Phys. Rev. E **83**, 036102 (2011).
[15] M. A. Muñoz, R. Juhász, C. Castellano, and G. Odor, Phys. Rev. Lett. **105**, 128701 (2010).
[16] G. Odor and R. Pastor-Satorras, Phys. Rev. E **86**, 026117 (2012).
[17] G. Odor, EPJ Web of Conferences **44**, 04005 (2013).
[18] G. Odor, Phys. Rev. E **87**, 042132 (2013).
[19] L. Isella, J. Stehlé, A. Barrat, C. Cattuto, J.-F. Pinton, and W. Van den Broeck, J. Theor. Biol. **271**, 166 (2011).
[20] L. A. Braunstein, S. V. Buldyrev, S. Havlin, and H. E. Stanley, Phys. Rev. E **65**, 056128 (2002).
[21] L. A. Braunstein, S. V. Buldyrev, R. Cohen, S. Havlin, and H. E. Stanley, Phys. Rev. Lett. **91**, 168701 (2003).
[22] C. Buono, C. Lagorio, P. A. Macri, and L. A. Braunstein, Physica A **391**, 4181 (2012).
[23] Z. Wu, C. Lagorio, L. A. Braunstein, R. Cohen, S. Havlin, and H. E. Stanley, Phys. Rev. E **75**, 066110 (2007).
[24] F. Vazquez, J. A. Bonachela, C. Lopez, and M. A. Muñoz, Phys. Rev. Lett. **106**, 235702 (2011).
[25] R. Martínez-García, F. Vazquez, C. López, and M. A. Muñoz, Phys. Rev E **85**, 051125 (2012).
[26] M. E. J. Newman, S. H. Strogatz, and D. J. Watts, Phys. Rev. E **64**, 026118 (2001).